

## An electrostatic micromechanical biosensor for electrical detection of label-free DNA

Ji-Min Choi, Sung-Up Hwang, Chang-Hoon Kim, Hyun-Ho Yang, Cheulhee Jung et al.

Citation: *Appl. Phys. Lett.* **100**, 163701 (2012); doi: 10.1063/1.3703764

View online: <http://dx.doi.org/10.1063/1.3703764>

View Table of Contents: <http://apl.aip.org/resource/1/APPLAB/v100/i16>

Published by the [American Institute of Physics](http://www.aip.org).

---

### Related Articles

Biofunctionalized AlGaIn/GaN high electron mobility transistor for DNA hybridization detection  
*Appl. Phys. Lett.* **100**, 232109 (2012)

Polymer translocation under time-dependent driving forces: Resonant activation induced by attractive polymer-pore interactions  
*JCP: BioChem. Phys.* **6**, 05B620 (2012)

Polymer translocation under time-dependent driving forces: Resonant activation induced by attractive polymer-pore interactions  
*J. Chem. Phys.* **136**, 205104 (2012)

High resolution resonant waveguide grating imager for cell cluster analysis under physiological condition  
*Appl. Phys. Lett.* **100**, 223701 (2012)

Accumulation mode field-effect transistors for improved sensitivity in nanowire-based biosensors  
*Appl. Phys. Lett.* **100**, 213703 (2012)

---

### Additional information on *Appl. Phys. Lett.*

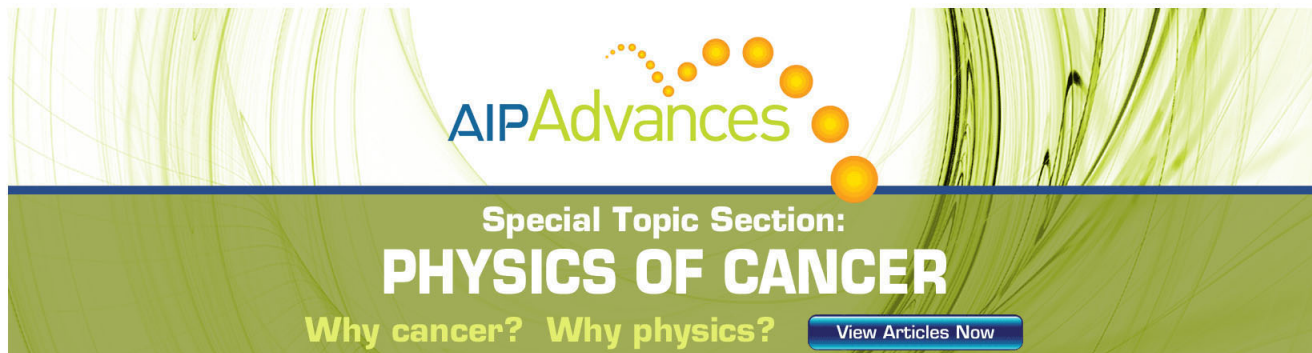
Journal Homepage: <http://apl.aip.org/>

Journal Information: [http://apl.aip.org/about/about\\_the\\_journal](http://apl.aip.org/about/about_the_journal)

Top downloads: [http://apl.aip.org/features/most\\_downloaded](http://apl.aip.org/features/most_downloaded)

Information for Authors: <http://apl.aip.org/authors>

## ADVERTISEMENT



**AIP Advances**

Special Topic Section:  
**PHYSICS OF CANCER**

Why cancer? Why physics? [View Articles Now](#)

## An electrostatic micromechanical biosensor for electrical detection of label-free DNA

Ji-Min Choi,<sup>1,a)</sup> Sung-Up Hwang,<sup>1,a)</sup> Chang-Hoon Kim,<sup>1</sup> Hyun-Ho Yang,<sup>1</sup> Cheulhee Jung,<sup>2</sup> Hyun Gyu Park,<sup>2</sup> Jun-Bo Yoon,<sup>1,b)</sup> and Yang-Kyu Choi<sup>1,b)</sup>

<sup>1</sup>Department of Electrical Engineering, Korea Advanced Institute of Science and Technology, 291 Daehak-ro, Yuseong-gu, Daejeon 305-701, South Korea

<sup>2</sup>Department of Chemical and Biomolecular Engineering, Korea Advanced Institute of Science and Technology, 291 Daehak-ro, Yuseong-gu, Daejeon 305-701, South Korea

(Received 23 February 2012; accepted 26 March 2012; published online 16 April 2012)

An electrostatic micromechanical biosensor is demonstrated for the label-free electrical detection of DNA, based on electrostatic actuation of a double-clamped micromechanical cantilever by driving gate electrodes to establish a current path through drain and source electrodes. Intrinsic charges in DNA alter surface charges on the gate by pre-charging concept and change the pull-in voltage ( $V_{PI}$ ), the voltage required to bring the suspended cantilever into contact with the drain electrode by induced electrostatic force. Its operation principle is verified by a numerical simulation and a capacitive model. The proposed biosensor represents a breakthrough for practical exploitation of electro-mechanical based sensors. © 2012 American Institute of Physics.

[<http://dx.doi.org/10.1063/1.3703764>]

Advances in the field of mechanical biosensors have notably accelerated recently.<sup>1–3</sup> The mechanical biosensors developed to date can be categorized as surface-stress sensors or dynamic-mode sensors. Surface-stress sensors measure the tiny deflection of a miniaturized mechanical device, whereas dynamic-mode sensors measure change of the oscillation resonance frequency. The predominant method for biomolecule detection in both categories of mechanical sensors is to employ an optical technique, whereby subtle deflection can be measured or the dynamic characteristics can be analyzed with the aid of a laser-assisted optical readout system.<sup>4–8</sup> The optical systems are advantageous in terms of high sensitivity as well as detection accuracy. However, the large size of the optical detection system induces constraints on the mechanical sensors when monolithic integration and implementation to portable sensors are considered. In addition, massive and multiplexed detection is also challenging owing to difficulties in the laser alignment.

To circumvent the aforementioned difficulties, capacitance<sup>9</sup> and piezoresistance<sup>10–12</sup> detection technologies have been investigated for mechanical biosensors as alternatives to optical detection. Since these methods do not require huge equipment such as a laser system, they mitigate the difficulties of monolithic integration for the readout system and external transducer, and they also enable electrical detection. Accordingly, these approaches are applicable to portable sensors. However, the resultant sensors are known to be susceptible to environmental interference and noise. A field-effect transistor (FET) embedded micromechanical biosensor<sup>13</sup> has also been developed. Although this sensor offers low noise, high sensitivity, and direct electric readout, the device was built on a silicon-on-insulator wafer, thus precluding the possibility of low-cost mass production.

Electrostatic micro-actuators based on micro-electromechanical system (MEMS) technology have also been applied for electronic and optical devices.<sup>14</sup> An electrostatic actuator is primarily composed of a cantilever-like suspended plate (movable), which is pulled in or out by the electrostatic force induced by an adjacent electrode (fixed). Here, a pull-in state refers to condition where the cantilever makes contact with a counter-electrode while a pull-out state implies that the cantilever pushes away from the counter-electrode. It has recently been verified that the pull-in voltage ( $V_{PI}$ ) of an electrostatic actuator can be altered by additional pre-charging of the counter-electrode.<sup>15,16</sup> In the same manner, it is plausible that  $V_{PI}$  can be changed when intrinsically charged particles such as biomolecules are immobilized on the counter-electrode.<sup>17</sup> By tracing the change of  $V_{PI}$ , electrostatic micro-actuators can be used as biosensors that combine an electronic and a mechanical switch, and consequently they can fully exploit the benefits of both electrical and mechanical detection. In this paper, applying this concept uniquely, we propose an innovative structured biosensor based on an electrostatic micro-actuator for electrical label-free DNA detection. Its operation is enabled by first bending the cantilever mechanically driven by the pull-in operation and then tracing and reading a signal electrically from the mechanical bending. The highly negative-charged phosphate backbones of the introduced DNA at a pre-designed area of the biosensor can produce a shift in the current-voltage ( $I$ - $V$ ) transfer characteristics via the aforementioned pre-charging mechanism. This concept was experimentally demonstrated and verified by numerical simulations. Its operating principle is comprehensively explicated by a simple capacitive model.

Figure 1(a) shows a schematic of the electrostatic micro-mechanical biosensor (referred to here as the sensor). A double-clamped cantilever (suspended beam), which is a structure supported by two anchors, has improved mechanical robustness against stiction, torsion, and deflection

<sup>a)</sup>J.-M. Choi and S.-U. Hwang contributed equally to this work.

<sup>b)</sup>Authors to whom correspondence should be addressed. Electronic addresses: jbyoon@ee.kaist.ac.kr and ykchoi@ee.kaist.ac.kr.

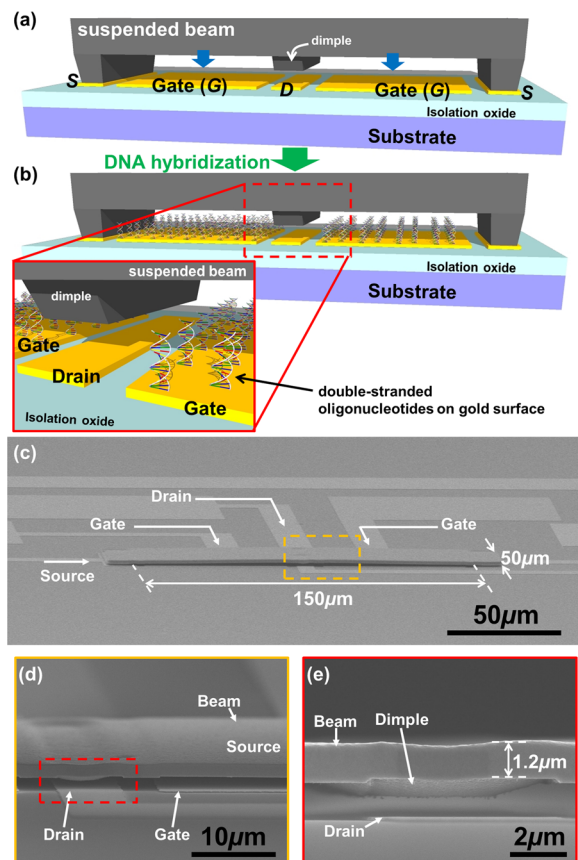


FIG. 1. (a) Illustration of the electrostatic micromechanical actuator device structure utilized for the biosensor. The suspended beam can be electrostatically pulled down (or pulled in) by the applied gate ( $G$ ) bias. At the pull-in voltage ( $V_{PI}$ ), the dimple of the beam contacts the drain ( $D$ ), thereby establishing a direct current path through between the drain and source ( $S$ ). (b) A schematic illustration of the sensor where the oligonucleotides are immobilized on the gate electrodes. The intrinsic negative charges from oligonucleotides on the gate surface alter the amount of electrostatic force acting on the cantilever in accordance with a pre-charging mechanism, thereby changing  $V_{PI}$ . (c)-(e) SEM images of the fabricated sensor: (c) a bird's-eye-view, (d) a close-up side view at the gap between the suspended beam and the electrodes, (e) a magnified side view at the gap between the dimple of the beam and the drain electrode.

compared with a single-clamped cantilever. In addition, a dimple structure is introduced to avoid physical contact between the gate electrode ( $G$ ) and the cantilever, especially when the dimple of the cantilever touches the drain electrode ( $D$ ). One of the electrodes of the micromechanical actuator structure is comprised of a plate micromechanically actuated by external voltage for pull-in or pull-out operation. The cantilever connected to the source electrode ( $S$ ) is electrostatically pulled in toward  $D$  by application of voltage to  $G$  ( $V_G$ ). At a certain applied bias known as the pull-in voltage ( $V_{PI}$ ), the electrostatic force between the cantilever and  $G$  becomes great enough to bring the dimple of the cantilever into contact with  $D$ . A direct electric current path through  $D$  and  $S$  is thereupon established. Drain current ( $I_D$ ) is therefore controlled by the amount of the applied bias to the gate electrode.

Several previous works have reported that the electrical characteristics of an electrostatic micro-actuator can be modified by employing an electrode pre-charging step.<sup>15,16</sup> Externally induced charges on a targeted electrode can then be detected by monitoring the change of the  $I$ - $V$  plot of the

micro-actuator. Figure 1(b) shows a schematic of the sensor device with oligonucleotides immobilized on  $G$ . It is worthwhile to note that DNA can also be immobilized onto  $D$ . However, DNA on  $G$  leads to variation of  $V_{PI}$ , because driving bias is applied to  $G$  rather than to  $D$ . Thus, DNA on  $D$  is not displayed in Fig. 1(b) for simplification. The intrinsic negative charges of oligonucleotides that are immobilized on  $G$  will alter  $I$ - $V$  characteristics of the sensor. Thus,  $V_{PI}$  to contact the cantilever onto  $D$  is accordingly changed by the amount of charges and charge polarity. When pull-in occurs, a conduction path between  $S$  and  $D$  is created, whereby  $I_D$  suddenly increases at the applied bias of  $V_{PI}$  as shown in Fig. 3(b). Because of the abrupt increment of  $I_D$  by "switching" behavior in the electrical characteristics, there is no reading error in tracing the change of  $V_{PI}$  at the proposed biosensor, whereas error or noise arises in reading the threshold voltage when using electrical-only FETs such as ion-sensitive field-effect transistors (ISFETs),<sup>18,19</sup> nanowire-based FETs,<sup>20,21</sup> etc.

The sensor is fabricated according to the process flow shown in the supplemental material.<sup>22</sup> Figure 1(c) shows bird's eye view SEM images of the fabricated sensor device. A rigid and reliable electrostatic micromechanical actuator was realized; negligible change in the pull-in voltage was observed during 20 successive measurements. A nominal cantilever has a length, width, and thickness of 150, 50, and 1.2  $\mu\text{m}$  (nickel thickness), respectively. The length and a width of  $G$  are 50 and 60  $\mu\text{m}$ , respectively. The measured gap displacement ( $g_G$ ) between the cantilever and  $G$  and the height of the dimple from SEM data (Figs. 1(d) and 1(e)) are approximately 1 and 0.7  $\mu\text{m}$ , respectively.

Conceptual demonstration of the proposed sensor is verified by the CoventWare<sup>TM</sup> simulation tool, as shown in Fig. 2. The dimensions of the simulated sensor are the same as those of the fabricated device. The 3-dimensional schematic model is designed as shown in Fig. 2(a). The simulation results are monitored by the change in the displacement (d) of the cantilever toward  $D$ . Figure 2(b) displays  $d$  as a function of  $V_G$ . In the simulation, negative electric bias is applied for device actuation, and consequently the external negative charges ( $|Q_B|$ ) from DNA lead to a reduction of the absolute value of the pull-in voltage ( $|V_{PI}|$ ) compared with the case of no external charges ( $Q_B = 0 \text{ C/cm}^2$ ).  $|V_{PI}|$  is read as the extrapolated  $d$  reaches 0.3  $\mu\text{m}$  (the value of the initial gap displacement  $g_D$  between the dimple and  $D$ ), which means the dimple touches  $D$ , i.e., pull-in occurs. As  $|Q_B|$  increases,  $|V_{PI}|$  tends to decrease as expected. Note that it works in the case when positive electric bias is applied, where  $V_{PI}$  tends to increase as the external negative charges ( $|Q_B|$ ) increases. This ambipolar behavior is attractive to improve the signal-to-noise ratio and confirm stability against the possible deformation of biomolecules during electrical biasing, through ambipolar biasing. Additionally, it is also inferred that there is a linear relationship between  $|V_{PI}|$  and  $|Q_B|$ , which is of importance in the calibration between a sensing metric such as  $V_{PI}$  and the quantity of biomolecules  $Q_B$ . These behaviors can be comprehensively understood by the simple capacitor models illustrated in Fig. 2(c). The conventional mechanical actuator can be considered as a capacitor with an air dielectric between two parallel

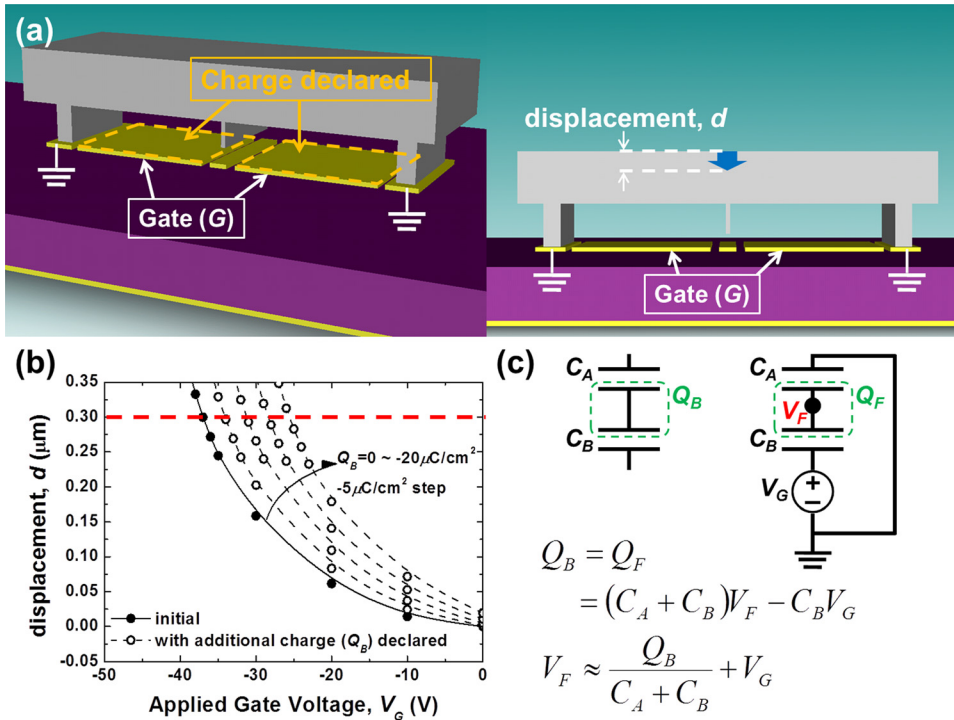


FIG. 2. Simulation results for a conceptual demonstration of the sensor. (a) 3-dimensional schematic model designed for the computational simulation. (b) The displacement of the suspended beam towards the drain is plotted as a function of the applied gate voltage.  $V_{PI}$  is the voltage when the dimple of the beam contacts the drain ( $d = 0.3 \mu\text{m}$ ). (c) Simplified capacitance model for a comprehensive analysis of the detection mechanism.

plates; one plate is a movable cantilever and the other is a fixed electrode with applied voltage. When charged molecules are bound to one of the two parallel plates, it can be considered as an additional floating plate with an external charge ( $Q_B$ ) introduced between the two plates. Therefore, this consideration can be modeled as two capacitors connected in series,  $C_A = \epsilon_{Air}/t_{Air}$  and  $C_B = \epsilon_{Bio}/t_{Bio}$ , where  $C_A$  and  $C_B$  are the normalized capacitance by the unit area for the air and the biomolecule dielectric, respectively. Here,  $\epsilon_{Air}$  and  $\epsilon_{Bio}$  are the permittivity of the air and the biomolecules, and  $t_{Air}$  and  $t_{Bio}$  are thickness of the air and the biomolecules, respectively. When  $V_G$  is applied to  $G$ , the amount of charges in the floating plate ( $Q_F$ ) is  $(C_A + C_B)V_F - C_B V_G$ . Since  $Q_B$  and  $Q_F$  are the same, the voltage of the floating plate ( $V_F$ ), which causes the cantilever to be pulled in, is expressed as

$$V_F = \frac{Q_B}{C_A + C_B} + \frac{C_B}{C_A + C_B} V_G \approx \frac{Q_B}{C_A + C_B} + V_G (\because C_B \gg C_A). \quad (1)$$

It is inferred that  $|V_F|$  is increased when polarities of  $Q_B$  and  $V_G$  are the same, thereby decreasing  $|V_{PI}|$ . Moreover, it is apparent from Eq. (1) that  $|V_{PI}|$  is increased when the polarities of  $Q_B$  and  $V_G$  are opposite. The simulation results, the trend of the shift in  $|V_{PI}|$  and the linear relationship between  $V_{PI}$  and  $Q_B$ , are directly deduced from the above equation.

For the experimental demonstration, thiolated-probe oligonucleotides are introduced to be immobilized on the Au surface of  $G$  to function as a DNA sensor. It is worthwhile to note that the Au electrodes in the sensor are connected to probing pads, which have a large parasitic area (approximately  $\sim 0.2 \text{ mm}^2$ ) including the interconnection area. Hence a tiny amount of DNA from the introduced solution can be effectively immobilized onto the area of  $G$  (the effective

sensing area) compared with the parasitic area, owing to the small fraction ratio of  $G$  relative to the parasitic area (approximately  $\sim 0.01$ ). This effect undesirably hinders the sensor from lowering the detection limit of DNA concentration on the sensor. Although not on par with the most sensitive sensors developed to date, DNA detection sensitivity of nM level is achieved in this study. However, by covering the parasitic area with a protective layer to prevent the DNA from being immobilized onto an unintended area, i.e., the parasitic area, the proposed sensor could feasibly detect even lower DNA concentrations. The detailed procedures of

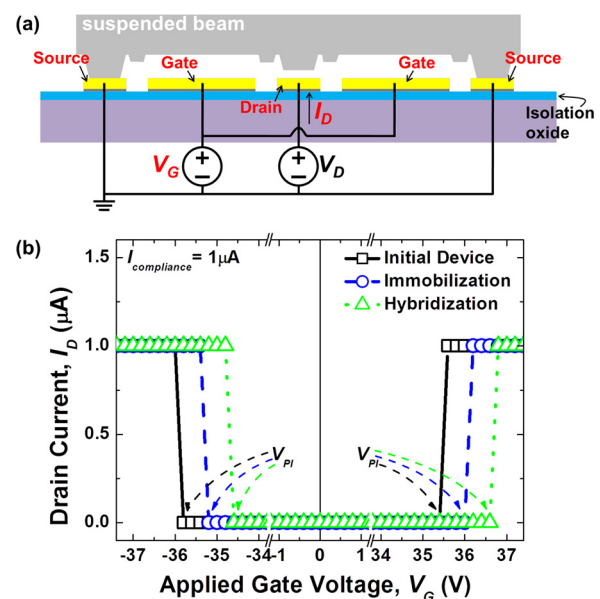


FIG. 3. (a) The experimental setup for electrical measurement of the sensor. (b) Typical measured transfer characteristics of the sensor for each step of the oligonucleotide binding process. The plot shifts to the right hand side ( $V_{PI}$  is increased) under negative and positive voltage domains due to the intrinsic negative charges of the oligonucleotides.

immobilization and hybridization of oligonucleotides are shown in the supplementary material.<sup>22</sup>

Figure 3(a) illustrates the measurement setup for evaluation of the sensor device in this work. The gate voltage ( $V_G$ ) is applied to  $G$  underneath the cantilever for electrostatic pull-in actuation. Electrical measurements for DNA detection were carried out by monitoring the change of the transfer characteristics ( $I_D$ - $V_G$ ) before and after each step of immobilization of the probe oligonucleotides and hybridization with the complementary oligonucleotides. Figure 3(b) shows typical experimental results for label-free DNA detection.  $I_D$  and  $V_{PI}$  are traced before any biological treatments (black), after immobilization of the probe oligonucleotide (blue), and after hybridization of the target oligonucleotide (green). As expected,  $V_{PI}$  sequentially increased after each procedure, i.e., immobilization of the thiol-terminated probe oligonucleotide (1  $\mu\text{M}$ ) and hybridization of the target oligonucleotide (1  $\mu\text{M}$ ). It should be noted that the proposed sensor works for ambipolar gate voltage, i.e., voltage ranging from negative to positive bias. The shift of  $|V_{PI}|$ , even at both negative and positive biasing, is in accordance with the aforementioned equations derived from simple capacitor models.

Figure 4 displays results of a statistical analysis of the DNA hybridization detection. All the data sets for one condition are obtained from 12 devices. There are two possible detection monitoring schemes: both polarities of the applied bias are investigated. A solid bar denotes the positive bias, while a lined bar represents the negative bias. Figure 4(a) shows the statistical analysis results of  $\Delta V_{PI}$  ( $=V_{PI,final} - V_{PI,initial}$ ) after each experimental procedure. First, the effect of deionized water on the initial device is investigated by dipping the device in a solution without any oligonucleotides. Negligible change in  $V_{PI}$  is observed, confirming the mechanical stability of the sensor structure; i.e., it is stiction-free. The device with the probe immobilized on  $G$  results in increment of  $V_{PI}$ . After hybridization of the complementary oligonucleotides to the immobilized probe oligonucleotides,  $V_{PI}$  is additionally increased compared to the device immobilized with probe oligonucleotides alone. This  $V_{PI}$  increment arises from the increased negative charges of the hybridized oligonucleotides, as expected. Furthermore, non-complementary target oligonucleotides are used as a control experiment to investigate the specificity of the DNA hybridization as a proof-of-concept of the functionality of the proposed sensor. No significant change is observed upon the introduction of the non-complementary oligonucleotides, although the feasibility of detecting of single-mismatched DNA pairs has not been established. This remains as further work. The detection capability is also investigated for various concentrations of the target oligonucleotide, as shown in Fig. 4(b). The concentration of the probe DNA is fixed at 1  $\mu\text{M}$ , while that of the target DNA is in a range of 1 nM to 1  $\mu\text{M}$ . The change of  $V_{PI}$  increases as the concentration increases and there is a linear relationship for both polarities of the applied bias, as verified by the abovementioned numerical simulations and the capacitance model.

In summary, an innovative structured biosensor based on electrostatic micromechanical behaviors was demonstrated for label-free DNA detection. The biosensor is composed of a suspended micromechanical cantilever that is electrostatically actuated by a driving gate electrode. At the

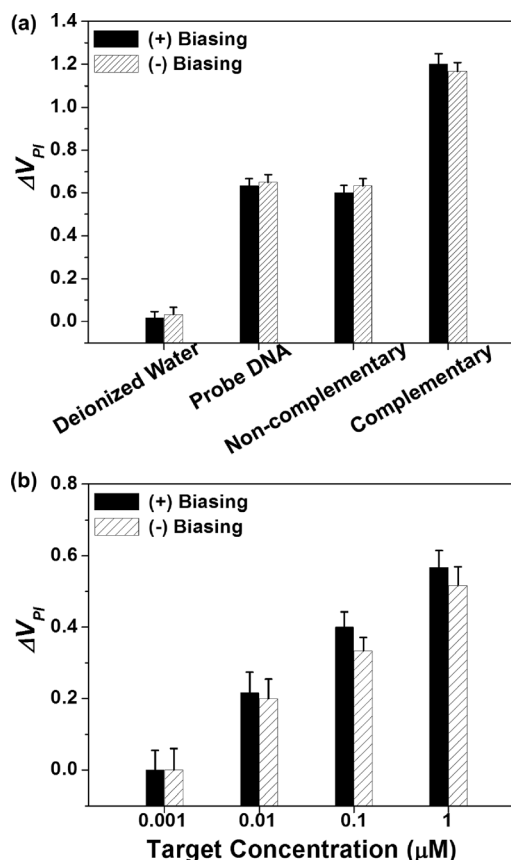


FIG. 4. (a) The modulation of the shift in pull-in voltage ( $\Delta V_{PI}$ ) for each status: the mechanical biosensor after being dipped in deionized water; after immobilization of the probe oligonucleotides; and after hybridization of the complementary target oligonucleotides. The specificity of the DNA hybridization is also investigated with non-complementary oligonucleotides. (b) Comparative results of  $\Delta V_{PI}$  of the sensor for various concentrations of complementary target oligonucleotides.

pull-in voltage, which is the applied voltage to contact the cantilever and the drain, a direct electric current path through the drain and source is established. The intrinsic negative charges arising from DNA on the gate surface were observed to alter the degree of influence of the electrostatic force on the cantilever by a pre-charging mechanism, thereby changing the pull-in voltage. The operational mechanism was verified by numerical simulations, and the underlying physics was comprehensively understood by a simple capacitive model developed. Experimental results demonstrated that the change in the pull-in voltage was induced by electrode pre-charging due to the intrinsic negative charges held by DNA. The proposed biosensor is expected to open an exploratory breakthrough for the detection of biomolecules.

This research was supported by the National Research and Development Program (NRDP, 2011-0002182) for the development of biomedical function monitoring biosensors and a grant from the National Research Foundation of Korea (NRF) funded by the Korean Ministry of Education, Science and Technology (MEST) (No. 2011-0020487). This work was also supported by the Smart IT Convergence System Research Center funded by the MEST (SIRC-2011-0031845).

<sup>1</sup>J. L. Arlett, E. B. Myers, and M. L. Roukes, *Nat. Nanotechnol.* **6**, 203 (2011).

<sup>2</sup>P. S. Waggoner and H. G. Craighead, *Lab Chip* **7**, 1238 (2007).

- <sup>3</sup>R. Raiteri, M. Grattarola, H.-J. Butt, and P. Skládal, *Sens. Actuators B* **79**, 115 (2001).
- <sup>4</sup>J. Fritz, M. K. Baller, H. P. Lang, H. Rothuizen, P. Vettiger, E. Meyer, H.-J. Güntherodt, Ch. Gerber, and J. K. Gimzewski, *Science* **288**, 316(2000).
- <sup>5</sup>J. Mertens, C. Rogero, M. Calleja, D. Ramos, J. A. Martín-Gago, C. Briones, and J. Tamayo, *Nat. Nanotechnol.* **3**, 301 (2008).
- <sup>6</sup>R. McKendry, J. Zhang, Y. Arntz, T. Strunz, M. Hegner, H. P. Lang, M. K. Baller, U. Certa, E. Meyer, H.-J. Güntherodt, and C. Gerber, *Proc. Natl. Acad. Sci. U.S.A.* **99**, 9783 (2002).
- <sup>7</sup>M. Su, S. Li, and V. P. Dravid, *Appl. Phys. Lett.* **82**, 3562 (2003).
- <sup>8</sup>T. Braun, M. K. Ghatkesar, N. Backmann, W. Grange, P. Boulanger, L. Letellier, H.-P. Lang, A. Bietsch, C. Gerber, and M. Hegner, *Nat. Nanotechnol.* **4**, 179 (2009).
- <sup>9</sup>C. L. Britton, Jr., R. L. Jones, P. I. Oden, Z. Hu, R. J. Warmack, S. F. Smith, W. L. Bryan, and J. M. Rochelle, *Ultramicroscopy* **82**, 17 (2000).
- <sup>10</sup>R. Mukhopadhyay, M. Lorentzen, J. Kjems, and F. Besenbacher, *Langmuir* **21**, 8400 (2005).
- <sup>11</sup>K. W. Wee, G. Y. Kang, J. Pakr, J. Y. Kang, D. S. Yoon, J. H. Park, and T. S. Kim, *Biosens. Bioelectron.* **20**, 1932 (2005).
- <sup>12</sup>P. A. Rasmussen, J. Thaysen, O. Hansen, S. C. Eriksen, and A. Boisen, *Ultramicroscopy* **97**, 371 (2003).
- <sup>13</sup>G. Shekhawat, S.-H. Tark, and V. P. Dravid, *Science* **311**, 1592 (2006).
- <sup>14</sup>J. G. Korvink and O. Paul, *MEMS: A Practical Guide to Design, Analysis, and Applications* (William Andrew, New York, 2006).
- <sup>15</sup>H.-H. Yang, J. O. Lee, and J.-B. Yoon, in *IEEE International Electron Device Meeting Technical Digest*, Washington DC, USA, 10–12 December 2007, pp. 439–442.
- <sup>16</sup>H.-H. Yang, D.-H. Choi, J. O. Lee, and J.-B. Yoon, *J. Micromech. Microeng.* **21**, 085012 (2011).
- <sup>17</sup>S.-U. Hwang, J.-M. Choi, H.-H. Yang, C.-H. Kim, C. Jung, H. G. Park, Y.-K. Choi, and J.-B. Yoon, in *IEEE MEMS Conference Technical Digest*, Cancun, Mexico, 23–27 January 2011, pp. 857–860.
- <sup>18</sup>P. Bergveld, *Sens. Actuators B* **88**, 1 (2003).
- <sup>19</sup>D. Gonçalves, D. M. F. Prazeres, V. Chu, and J. P. Conde, *Biosens. Bioelectron.* **24**, 545 (2008).
- <sup>20</sup>Z. Gao, A. Agarwal, A. D. Trigg, N. Singh, C. Fang, C.-H. Tung, Y. Fan, K. D. Buddharaju, and J. Kong, *Anal. Chem.* **79**, 3291 (2007).
- <sup>21</sup>J. Hahn and C. M. Lieber, *Nano Lett.* **4**, 51 (2004).
- <sup>22</sup>See supplementary material at <http://dx.doi.org/10.1063/1.3703764> for the detail of the fabrication process of the micromechanical sensor.